Modeling interdependencies in multi-sectoral critical infrastructure systems: evolving the DMCI approach

Luca Galbusera

European Commission, Joint Research Centre (JRC), Ispra, Italy

Paolo Trucco

Politecnico di Milano, Department of Management, Economics and Industrial Engineering, Milan, Italy

Georgios Giannopoulos*

European Commission, Joint Research Centre (JRC), Ispra, Italy

Abstract

The adequate functioning of critical infrastructures is crucial for sustaining the development of today's societies and economies. It is a priority, therefore, to foster our understanding of such systems and ability to assess interdependencies, vulnerabilities, and resilience. Starting from the DMCI (Dynamic functional Modelling of vulnerability and interoperability of Critical Infrastructure systems) framework proposed in [1], in this paper we present an evolved formalism (DMCI-e). This introduces novel modeling features and enhances applicability while keeping the original focus on a dynamic and network-centric characterization of disservice. A key objective is to respond to the need, expressed by policy-makers and critical infrastructure regulators, for sector-agnostic and multi-granular infrastructure models for the estimation of service supply capabilities and response during and after disruptive events.

Keywords: critical infrastructures; interdependencies; cascading effects; dynamic modeling; simulation

1. Introduction

Modern Critical Infrastructures (CIs) are, in many cases, highly interconnected and mutually dependent systems [2, 3, 4, 5, 6, 7, 8]. This gives opportunities for a more efficient exploitation of resources and orchestration of services, yet it may sometimes allow existing vulnerabilities to escalate and new ones to emerge. Under specific circumstances, even a relatively small malfunction affecting a single component may result in broad-scale and long-lasting impacts, sometimes through cascading sequences proving hard to predict and prevent [9, 10].

Various policy instruments, at the EU level, displayed a fundamental effort to address these issues [11]. Notable examples are Council Directive 2008/114/EC ("ECI Directive") [12] and Commission Staff Working Document SWD(2013)-318-final [13], which stressed the need to improve CI resilience, address interdependencies, and govern cascading effects. The latter document also put forward the implementation of pilot projects targeting the assessment of impacts on CIs at the European level by several threats. Moreover, Directive (EU) 2016/1148 ("NIS Directive") [14], focusing on operators of essential services and digital service providers, established measures meant to enhance resilience and called for a deep understanding of interdependencies with an emphasis on the cyber-sphere.

Ensuring the resilience of modern CIs also requires substantial scientific backing, for instance, to identify and model vulnerabilities, interdependencies and cascading effects at the system-of-systems level [15]. This need motivates the interest of the community in CI complexity, as well as in the development of appropriate tools to support decisions and policy-making. Review paper [16] witnesses the breadth of methodologies and simulation models emerging in this domain. Accordingly, when evaluating the different instruments at disposal, it can be of interest to compare how they trade

*Corresponding author.
E-mail: georgios.giannopoulos@ec.europa.eu.

off the level of modeling detail against the spectrum of sectors and interdependence classes accounted for.

In this paper, in particular, we take as a reference the DMCI (Dynamic functional Modelling of vulnerability and interoperability of Critical Infrastructure systems) approach from [1]. DMCI introduces a dynamic perturbation characterization of interdependent CIs, portrayed as a network of nodes supplying services to both their neighbors and to end customers, in response to specified demand profiles. In turn, the ability of nodes to deliver service generally relies on both internal processes and the availability of upstream supply. DMCI's service-oriented representation conceptually replaces flow-based formulations expressed at the physical level and involving, for instance, power in electrical grids, gas in distribution pipelines, or vehicles on roads. These features make DMCI a sector-agnostic modeling framework, whose relationships with various kinds of interdependence (especially considering the physical, cybernetic, geographic, and logical types) have been addressed in [1]. Further developments of the technique, including a sample application to a pilot case involving the transportation and power transmission infrastructure, can be found in [17].

The present contribution aims to introduce an evolved DMCI approach (DMCI-e), which both upgrades modeling capabilities and increments applicability while maintaining moderate data requirements. Also in case, beyond demand perturbation, key mechanisms leading to disservice include functional integrity loss (reduction of a node's intrinsic service capacity) and inoperability (reduction of a node's effective service capacity due to network disservices). At the same time, we introduce some novel features, such as

- an array of node types (including service source nodes, linear service nodes, and fixed-proportion service nodes), to qualify how services are sourced and transformed throughout the system, as well as how demand is handled and dispatched therein;
- multiple demand shift criteria (in particular an internal and an external mechanism), each operating according to a specific logic and potentially across distinct node combinations, with the ability to redistribute demand based on need and service replaceability considerations.

These factors allow for higher flexibility in describing and simulating multi-sectoral interdependent CI systems, analyzing complex cascading effects, and assessing different demand reconfiguration patterns that the system could manifest when facing a critical event.

The remainder of the paper is organized as follows: in Section 2 we briefly review key categorizations of state-of-the-art CI interdependence modeling techniques and discuss how DMCI-e relates to them; Section 3 introduces DMCI-e's baseline representation of CI networks in terms of demand, supply, and node types; Section 4 details the architecture of the DMCI-e model, which includes a service module and a demand module; in Section 5 we propose illustrative examples, and some concluding remarks follow. For ease of reference, a list of symbols used throughout the paper is provided in Table 1.

symbol	description
(network structure)	
n	number of nodes
$\mathcal{G}^s = (\mathcal{N}, \mathcal{E}^s)$	service graph
$\mathcal{G}^{ES} = (\mathcal{N}, \mathcal{E}^{ES})$	external demand shift (ES) graph
$\mathcal{G}^{IS} = (\mathcal{N}, \mathcal{E}^{IS})$	internal demand shift (IS) graph
$\mathcal{N}_i^-(\mathcal{G}), \mathcal{N}_i^+(\mathcal{G})$	sets of in- and out-neighbors of node i in graph $\mathcal{G}$
ν_i	node i's type
(service)	
$s_i(t)$	node i's service supply
$s_i^f(t), s_i^p(t), s_{(i,j)}(t)$	node i's final service supply, process service supply, service supply to node j
A	service aggregation matrix
$\bar{s}_i^{MAX}$	node i's nominal service capacity
$\bar{s}_i^F(t), x_i^F(t)$	node i's intrinsic service capacity, functional integrity loss
$\mathcal{N}^F, \mathcal{T}_i^F$	set of impacted nodes, node i's threat impact times
τ_i^b, τ_i^r	node i's buffering time, recovery response time
ψ_i^F	node i's regime functional integrity reduction
$\bar{s}_i^I(t), x_i^I(t)$	node i's effective service capacity, inoperability
$\bar{l}_{(i,j)}$	edge (i, j)'s inoperability propagation threshold
$\tau_{(i,j)}^b, \tau_{(i,j)}^r$	edge (i, j)'s buffering time, recovery response time
$\mu_{(i,j)}$	edge (i, j)'s inoperability dependence sensitivity
(demand)	
$d_i^{I,*}(t)$	node i's reference final service demand
$d_i^I(t)$	node i's final service demand
k_i^{ES}, k_i^{IS}	node i's ES-/IS-type demand shift ratio
τ_i^{ES}, τ_i^{IS}	node i's ES-/IS-type disservice tolerance time
$D^{ES}, D^{IS}(t)$	ES-/IS-type demand shift matrix
$d_i(t)$	node i's service demand
$d_i^f(t), d_i^p(t), d_{(i,j)}(t)$	node i's final demand, process demand, demand by node j
Δ	demand disaggregation matrix
$\bar{d}_i^F(t)$	node i's intrinsic capacity-constrained demand
(disservice and service margin)	
$l_i(t), m_i(t)$	node i's disservice, service margin
$l_{(i,j)}(t)$	edge (i, j)'s disservice

Table 1: selected notation used in the DMCI-e model formulation.

2. State-of-the-art CI interdependence modeling: categorizations and framing of DMCI-e

In recent years, several researchers put considerable effort into enhancing our ability to understand and assess interdependencies and vulnerabilities in complex CI systems. Available modeling and simulation approaches engage different scientific disciplines, such as

complex network theory, physical network modeling, network economics [18, 19, 20, 21, 22, 23, 24, 25, 26, 27, 28, 29, 30]. As far as the selection of an appropriate technique is concerned, the analytic insights provided by different methods drastically depend on the semantics of the adopted formalism. Moreover, a relevant driver is the choice of adequate levels of granularity and accuracy, as needed to guarantee a suitable balance between quality of results, computational time, and data requirements.

Reference [31] points out that *"the analysis of CIs cannot be carried out only with classical methods of system decomposition and logic analysis; a framework is needed to integrate a number of methods capable of viewing the complexity problem from different perspectives (topological and functional, static and dynamic), under the existing uncertainties"*. In this sense, even if there is no one-size-fits-all solution, certainly it is to the interest of the community to develop simulation tools proving to be versatile and reliable for a wide gamut of problems, decision-making processes, and scenarios.

Review [16] offers a comprehensive overview of emerging modeling and simulation techniques for interdependent CI systems. These are organized into six categories:

- empirical approaches;
- agent-based approaches;
- system dynamics-based approaches;
- economic theory-based approaches;
- network-based approaches;
- other approaches e.g. based on hierarchical holographic modeling (HHM), high level architecture (HLA), Petri-net (PN), dynamic control system theory (DCST), and Bayesian network (BN) methods.

The same paper contains an evaluation of the types of interdependencies addressable by the mentioned modeling categories and some subcategories, referring to the well-known framework from [9]. Besides, input data quantity and accessibility, computational costs, maturity and resilience aspects are accounted for. See also [32] for a recent classification and comparison of CI protection modeling tools according to purpose and technical approach, employing the above-listed categories.

To the scope of our discussion, we can also consider the following grouping:

- *topology-based methods* (e.g. [33, 34, 35, 36, 37, 38, 39, 40]), that are primarily used for identifying critical nodes and arcs in complex networks and carrying out vulnerability analyses;
- *flow-based methods* (e.g. [35, 41, 42, 43, 40]), wherein the main objective is to study the dynamics of cascading effects and to assess and rank the expected benefits of alternative mitigation actions;
- *hybrid methods* (e.g. [44, 45, 46, 47, 48, 49, 50]), generally adopted in the attempt to build larger simulation models, where different physical models of specific CI systems and/or decision criteria can be integrated to simulate the mitigation of cascading failures and the dynamics of the recovery process.

Within such landscape, the DMCI-e formalism, similarly to DMCI, can be qualified as a flow-based framework to network modeling oriented to services. Indeed, [16] mentions DMCI among the flow-based methods, a subcategory of the network-based approaches wherein *"nodes and edges constructing the infrastructure topologies have the capacities to produce, load and deliver the services"*.

Another relevant attribute of both DMCI and DMCI-e is that, therein, CI systems are modeled at a functional level, through a set of nodes delivering services and dynamically adapting to variable demand, under evolving operational conditions. Various types of dependencies are encompassed and different nodes can belong to the same CI as well as to different CI systems. From this perspective, we refer the reader to the distinction between physical, functional and socio-economic dimensions discussed in [1].

As argued in the latter reference and further recent literature, methodologies that model the CI system-of-systems from a functional point of view seem to display the highest potential to take into proper consideration a wider spectrum of interdependencies, while mitigating computational burden and meeting data accessibility constraints [51, 52, 53, 40]. To fully tackle system complexity, such approaches could also be integrated into larger model federations (multi-formalism approach), for instance by receiving input data directly from physical models of different CI systems, or feeding their output into other algorithms implementing agent-based or economic theory-based models.

3. DMCI-e's service-oriented representation of networked CIs

In this section, we illustrate the baseline representation of networked CIs exploited in the DMCI-e model formulation. We start by introducing *service graph* $\mathcal{G}^s = (\mathcal{N}, \mathcal{E}^s)$, a simple graph where $\mathcal{N} = \{1, \dots, n\}$ is the set of nodes and $\mathcal{E}^s \subset \mathcal{N} \times \mathcal{N}$ the set of edges. Denote by $\mathcal{N}_i^-(\mathcal{G}^s) = \{h \in \mathcal{N} : (h,i) \in \mathcal{E}^s\}$ the set of in-neighbors of i and by $\mathcal{N}_i^+(\mathcal{G}^s) = \{j \in \mathcal{N} : (i,j) \in \mathcal{E}^s\}$ that of its out-neighbors. The structure of the graph expresses demand-service relationships in place across the network, wherein nodes in $\mathcal{N}_i^-(\mathcal{G}^s)$ are service suppliers to node i and the latter, in turn, supplies nodes in $\mathcal{N}_i^+(\mathcal{G}^s)$. In addition to that, some nodes also serve final demand, determined by end customers and driving internal demand.

Based on the introduced service graph, next we discuss the relevant node demand and supply terms. In particular, we detail how those quantities are aggregated and disaggregated as a function of the service network's attributes and topology.

3.1. Demand aggregation and supply disaggregation

Considering a time interval $\mathcal{T} \subseteq \mathbb{N}_0$ for our analysis, the operational objective of each node $i \in \mathcal{N}$ is to supply, $\forall t \in \mathcal{T}$, a *service demand* profile $d_i(t) \geq 0$ expressed as follows:

$$d_i(t) = d_i^f(t) + d_i^p(t) \tag{1}$$

where functions $d_i^f(\cdot),\ d_i^p(\cdot) : \mathcal{T} \mapsto \mathbb{R}_{\geq 0}$ denote *final* (end customer-to-node) and *process* (node-to-node) *demand*, respectively. In turn, the latter term is articulated as

$$d_i^p(t) = \sum_{j \in \mathcal{N}_i^+(\mathcal{G}^s)} d_{(i,j)}(t) \tag{2}$$

where $d_{(i,j)}(\cdot) : \mathcal{T} \mapsto \mathbb{R}_{\geq 0}$ defines *node i's demand by node j*.

Similarly, each node's *service supply* in response to demand will be described by $s_i(t) \in [0, d_i(t)]$, $\forall t \in \mathcal{T}$, fulfilling relationship

$$s_i(t) = s_i^f(t) + s_i^p(t) \tag{3}$$

Herein, *final* and *process service supply* terms $s_i^f(\cdot),\ s_i^p(\cdot) : \mathcal{T} \mapsto \mathbb{R}_{\geq 0}$ determine how quotas of the available supply by node i is are allotted to end customers and downstream nodes, with

$$s_i^p(t) = \sum_{j \in \mathcal{N}_i^+(\mathcal{G}^s)} s_{(i,j)}(t) \tag{4}$$

In the latter formula, $s_{(i,j)}(\cdot) : \mathcal{T} \mapsto \mathbb{R}_{\geq 0}$ is *node i's service supply to node j*. We assume that, in order to allocate $s_i(t)$, a demand-proportional rationing scheme is implemented, i.e.

$$s_i^f(t) = \frac{d_i^f(t)}{d_i(t)} s_i(t) \tag{5}$$

$$s_{(i,j)}(t) = \frac{d_{(i,j)}(t)}{d_i(t)} s_i(t),\ \forall j \in \mathcal{N}_i^+(\mathcal{G}^s) \tag{6}$$

if $d_i(t) > 0$ and zero otherwise. The latter rules aim at ensuring both $s_i^f(t) = d_i^f(t)$ and $s_{(i,j)}(t) = d_{(i,j)}(t)$, $\forall j \in \mathcal{N}_i^+(\mathcal{G}^s)$, when $s_i(t) = d_i(t)$.

On the other side, as detailed in the DMCI-e model formulation that follows, some circumstances may render it unfeasible to ensure the target service levels. Accordingly, introduce *node disservice*

$$l_i(t) = d_i(t) - s_i(t),\ \forall i \in \mathcal{N} \tag{7}$$

and *edge disservice*

$$l_{(i,j)}(t) = d_{(i,j)}(t) - s_{(i,j)}(t),\ \forall (i,j) \in \mathcal{E}^s \tag{8}$$

Observe that, by definition, the mentioned disservice variables are non-negative.

3.2. Supply aggregation and demand disaggregation

Above we focused on the way each node interacts with the rest of the system by aggregating demand and allocating the available services. As a next step, we now address more in details a node's internal operation.

Different criteria may determine how a node pools internal and external resources to convey the service aimed for, as well as how it generates demand towards upstream nodes. To describe that, first introduce a *service aggregation matrix* $A = [A_{(h,i)}]_{h,i \in \mathcal{N}}$ with $A_{(h,i)} > 0$ if $(h,i) \in \mathcal{E}^s$ and $A_{(h,i)} = 0$ otherwise. Herein, $A_{(h,i)}$ denotes a conversion factor applied to service $s_{(h,i)}(\cdot)$ in the context of node i's aggregated service, $\forall (h,i) \in \mathcal{E}^s$. Exploiting this definition, to capture some of the diversity found in practice we classify the following node types:

- *service source node* (α-node): this is the case of nodes $i \in \mathcal{N}$ such that $\mathcal{N}_i^-(\mathcal{E}^s) = \emptyset$, thus the node's ability to deliver service entirely relies on its internal capabilities and processes;
- *linear service node* (β-node): in this case, $\mathcal{N}_i^-(\mathcal{E}^s) \neq \emptyset$ and the node performs a pure linear transformation over the services provided in input, i.e. $s_i(t) = \sigma_i^\beta\left([s_{(h,i)}(t)]_{h \in \mathcal{N}_i^-(\mathcal{G}^s)}\right)$ with

$$\sigma_i^\beta\left([s_{(h,i)}(t)]_{h \in \mathcal{N}_i^-(\mathcal{G}^s)}\right) = \sum_{h \in \mathcal{N}_i^-(\mathcal{G}^s)} A_{(h,i)} s_{(h,i)}(t) \tag{9}$$

- *fixed-proportions service node* (γ-node): also in this case $\mathcal{N}_i^-(\mathcal{E}^s) \neq \emptyset$, while individual input services are considered as non-substitutable factors, and the associated transformation is expressed as $s_i(t) = \sigma_i^\gamma\left([s_{(h,i)}(t)]_{h\in\mathcal{N}_i^-(\mathcal{G}^s)}\right)$ with

$$\sigma_i^\gamma\left([s_{(h,i)}(t)]_{h\in\mathcal{N}_i^-(\mathcal{G}^s)}\right) = \min_{h\in\mathcal{N}_i^-(\mathcal{G}^s)} A_{(h,i)}s_{(h,i)}(t) \quad (10)$$

Nodes of different types may coexist within a given network and even contribute to the representation of a single infrastructure component, depending on its complexity and on the target granularity level.

Remark 1. ***(Node types)*** *The introduction of β and γ node types allows flexibility in representing networked service aggregation. A β-type node may describe, for instance, a multi-seller logistic chain or an electrical distribution network depending on the service of multiple transformation cabins. On the other side, an example of γ-type node may be a manufacturing production chain working at constant mix or a railway station needing the availability of both the transportation infrastructure and the electrical distribution network to operate. Finally, observe that the introduced β- and γ-type supply aggregation functions have analogies with the linear- and Leontief-type production functions found in economics [54].*

Having outlined different node types and service aggregation modes, we can now focus on demand disaggregation. To this end, introduce a *demand disaggregation matrix* $\Delta = [\Delta_{(h,i)}]_{h,i\in\mathcal{N}}$ with $\Delta_{(h,i)} > 0$ if $(h,i) \in \mathcal{E}^s$ and $\Delta_{(h,i)} = 0$ otherwise. On this basis, we assign $d_{(h,i)}(t) = \Delta_{(h,i)}d_i(t)$. Therefore, from (1) and (2),

$$d_i(t) = d_i^f(t) + \sum_{j\in\mathcal{N}_i^+(\mathcal{G}^s)} \Delta_{(i,j)}d_j(t) \quad (11)$$

or equivalently, in vector form,

$$(I - \Delta)\, d(t) = d^f(t) \quad (12)$$

with $d(t) = [d_1(t), \ldots, d_n(t)]'$, $d^f(t) = [d_1^f(t), \ldots, d_n^f(t)]'$. From now on, we assume that $(I-\Delta)$ is non-singular, so that $d(t)$ is uniquely assigned from $d^f(t)$.

Next, we introduce a plausible method to construct Δ, i.e. a formulation ensuring $\sigma_i^{\nu_i}\left([d_{(h,i)}(t)]_{h\in\mathcal{N}_i^-(\mathcal{G}^s)}\right) = d_i(t)$ if $\nu_i \in \{\beta,\gamma\}$, $\forall i \in \mathcal{N}$, where ν_i is *node i's type*. To this end, consider the following node type-specific definitions:

- β-node:

$$\Delta_{(h,i)}^\beta = \left(\sum_{k\in\mathcal{N}_i^-(\mathcal{G}^s)} A_{(k,i)}\right)^{-1},\ \forall h \in \mathcal{N}_i^-(\mathcal{G}^s) \quad (13)$$

- γ-node:

$$\Delta_{(h,i)}^\gamma = (A_{(h,i)})^{-1},\ \forall h \in \mathcal{N}_i^-(\mathcal{G}^s) \quad (14)$$

On the basis of (13) and (14), define

$$\Delta_{(h,i)} = \begin{cases} \Delta_{(h,i)}^{\nu_i} & \text{if } h \in \mathcal{N}_i^-(\mathcal{G}^s) \wedge \nu_i \in \{\beta,\gamma\} \\ 0 & \text{otherwise} \end{cases} \quad (15)$$

$\forall h, i \in \mathcal{N}$. Herein, the above-mentioned non-singularity property is assumed to be guaranteed by virtue of a proper choice of node types and service aggregation factors.

Observe that no upper bounds have been imposed so far on variables $s_i(t)$ other than $s_i(t) \leq d_i(t)$, $\forall i \in \mathcal{N}$. Correspondingly, it is possible to verify that all node types allow ensuring $s_i(t) = d_i(t)$ under (15); in the case of type β (resp. γ), this can be verified considering (9) and (13) (resp. (10) and (14)) in conjunction with (6). Differently, the DMCI-e module we will consider next introduces a richer representation of service constraints and their toppling consequences in the network, together with additional features related to demand. Finally notice that, to the scope of this paper, we do not consider competitive behaviors in the definition of process demand terms towards the allocation of the available services.

4. Modular structure of the DMCI-e model

DMCI-e exploits the concepts of service network, node types, service demand and supply proposed above to represent and analyze perturbations and their propagation in infrastructural systems-of-systems. The objective of this section is, therefore, to accommodate such kind of analysis by reframing the baseline formulation from Section 3. This operation is accomplished by introducing a dynamical characterization which takes into account constraints affecting the ability of the system to match service demand and supply. The mentioned constraints can derive from both internal and external factors, as detailed below.

From the architectural viewpoint, two main components are in place to evaluate the joint effect of impacting threats, (inter)dependencies and countermeasures:

- the *service module*, which aims at expressing the degradation and recovery of service levels occurring in time as a function of the status of the overall network and its parts;

- the *demand module*, which determines how demand is assigned to and transferred among nodes, based on factors such as the residual service capabilities of the system in the aftermath of a shock.

See Figure 1 for a diagram about the DMCI-e architecture outlined so far as well as the internal structure of each module, that will be detailed throughout the rest of this section.

4.1. Service module

In the DMCI-e representation, each node $i \in \mathcal{N}$ is characterized by a *nominal service capacity* $\bar{s}_i^{MAX} > 0$, which limits the maximum service level it can output even under nominal operating conditions. In addition to that, a node's ability to respond to demand may be undermined by both the direct effect of threats it is impacted by, and the unavailability of upstream services. To take this duality into account, we introduce the following concepts:

- *functional integrity loss*, affecting the intrinsic ability of a node to deliver service and, potentially, the process demand it generates;

- *inoperability*, further conditioning a node's capability to fulfill demand due to network disservices.

Such aspects are handled by distinct submodules leading to the attribution of intrinsic service capacity $\bar{s}_i^F(t)$ and, through the interaction with the demand module, effective service capacity $\bar{s}_i^I(t)$, $\forall i \in \mathcal{N}$ and $\forall t \in \mathcal{T}$. These are dynamically assigned upper bound constraints on supply. Observe that in this paper we do not consider perturbations to the technical matrices A and Δ. The service module also includes the computation of service losses and service margins.

Next, we analyze more in details each submodule.

4.1.1. Functional integrity loss

In our representation, *functional integrity loss* $x_i^F(\cdot) : \mathcal{T} \mapsto [0, 1]$, $\forall i \in \mathcal{N}$, determines the fraction of a node's nominal service capacity $\bar{s}_i^{MAX}$ that is not available in time due to node-specific perturbations. Accordingly, we compute its *intrinsic service capacity* as

$$\bar{s}_i^F(t) = \bar{s}_i^{MAX}\left(1 - x_i^F(t)\right) \tag{16}$$

As such, functional integrity loss can restrain a node's maximum service capabilities, which by assumption cannot be compensated through increased service levels by upstream nodes. In this sense, $\bar{s}^F(\cdot)$ is exploited towards the definition of intrinsic capacity-constrained demand $\bar{d}^F(\cdot)$ and associated edge demand, see Subsection 4.2.2. Through such demand terms, $\bar{s}^F(\cdot)$ also affects the forward propagation of disservice in terms of inoperability.

Next, we introduce a dynamical model that can be used to assign functional integrity loss over time as a function of key node and perturbation attributes. In order to do so, first define the *set of impacted nodes* $\mathcal{N}^F \subseteq \mathcal{N}$ and the associated unbuffered switching signal

$$\rho_i^F(t) = \begin{cases} 0 & \text{if } t \in \mathcal{T}_i^F \\ 1 & \text{otherwise} \end{cases} \tag{17}$$

$\forall i \in \mathcal{N}^F$, where $\mathcal{T}_i^F \subseteq \mathcal{T}$ is the *set of threat impact times*. Based on the latter formula, also introduce the buffered switching signal

$$\theta_i^F(t) = \begin{cases} 0 & \text{if } \left(\begin{smallmatrix}(\theta_i^F(t^-)=1)\wedge \\ (\rho_i^F(t-\tau)=0,\ \forall\tau\in[0\ ..\ \tau_i^b])\end{smallmatrix}\right) \\ 1 & \text{if } \left(\begin{smallmatrix}(\theta_i^F(t^-)=0)\wedge \\ (\rho_i^F(t-\tau)=1,\ \forall\tau\in[0\ ..\ \tau_i^r])\end{smallmatrix}\right) \\ \theta_i^F(t^-) & \text{otherwise} \end{cases} \tag{18}$$

$\forall i \in \mathcal{N}^F$, where $t^- = t - 1$. Herein, $\theta_i^F(t) = 0$ and $\theta_i^F(t) = 1$ denote the failure and recovery/normal operation modes, respectively. Moreover,

- $\tau_i^b \in \mathbb{N}_0$ (*node buffering time*) determines the time interval over which a node can withstand continuous perturbation before the activation of the failure mode (e.g. thanks to the presence of inventories, backup solutions or other kinds of buffering mechanisms);

- $\tau_i^r \in \mathbb{N}_0$ (*node recovery response time*) indicates the time interval a node has to stay unaffected by the perturbation before recovery is triggered (e.g. in order to set up countermeasures).

Both quantities may depend on the nature and intensity of the threat affecting the system. Also, introduce the following definitions, $\forall i \in \mathcal{N}^F$:

- *F-type intensity modulation*, expressed as

$$\psi_i^F(t) = \begin{cases} \bar{\psi}_i^F & \text{if } \theta_i^F(t) = 0 \\ 0 & \text{otherwise} \end{cases} \tag{19}$$

  where $\bar{\psi}_i^F \in [0, 1]$ characterizes the *regime functional integrity reduction* imposed by the perturbation;

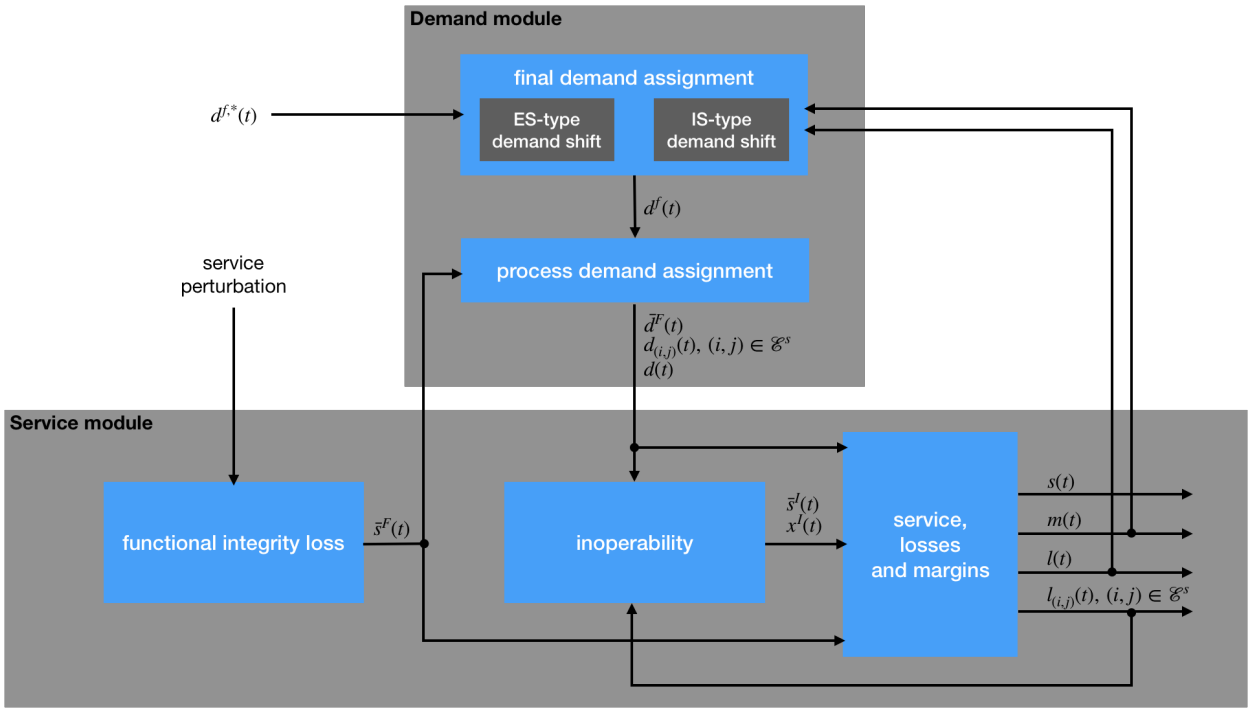

Figure 1: DMCI-e model architecture (service and demand modules, associated submodules).

- *F-type time modulation*, described by a set of continuous, monotone decreasing functions $\xi^F_{i,k}(\cdot) : \mathbb{R} \mapsto \mathbb{R}$ with $|\xi^F_{i,k}(x)| \in [0, |x|]$, for $k = 0, 1$ and $\forall x \in \mathbb{R}$.

Then, $\forall t \in \mathcal{T}$, functional integrity loss will be computed as

$$x^F_i(t) = x^F_i(t^-) + \xi_{i,\theta^F_i(t^-)}\left(x^F_i(t^-) - \psi^F_i(t^-)\right) \tag{20}$$

if $i \in \mathcal{N}^F$, while $x^F_i(t) = 0$ otherwise.

4.1.2. Inoperability

Node inoperability $x^I_i(\cdot) : \mathcal{T} \mapsto [0, 1]$, $\forall i \in \mathcal{N}$, describes the reduction to a node's demand supply capability deriving from the lack of services requested from in-neighbors, if any. The computation of node inoperability is based on *edge inoperability* variables $x^I_{(h,i)}(\cdot) : \mathcal{T} \mapsto [0, 1]$, $\forall (h, i) \in \mathcal{E}^s$. These, on the basis of the edge demand terms generated by the demand module, determine edge supply terms

$$\bar{s}^I_{(h,i)}(t) = d_{(h,i)}(t)\left(1 - x^I_{(h,i)}(t)\right) \tag{21}$$

$\forall (h, i) \in \mathcal{E}^s$, and ultimately the *effective service capacity*

$$\bar{s}^I_i(t) = \begin{cases} \bar{d}^F_i(t) & \text{if } \nu_i = \alpha \\ \sigma^{\nu_i}_i\left(\left[\bar{s}^I_{(h,i)}(t)\right]_{h \in \mathcal{N}^-_i(\mathcal{G}^s)}\right) & \text{if } \nu_i \in \{\beta, \gamma\} \end{cases} \tag{22}$$

$\forall i \in \mathcal{N}$, where $\bar{d}^F_i(t)$ is the intrinsic capacity-constrained demand of node i, assigned by the demand module, while $\sigma^\beta_i(\cdot)$ and $\sigma^\gamma_i(\cdot)$ are defined as in (9) and (10), respectively.

When $\bar{d}^F_i(t) \neq 0$, we can finally express node i's *inoperability* at time t as

$$x^I_i(t) = 1 - \frac{\bar{s}^I_i(t)}{\bar{d}^F_i(t)} \tag{23}$$

so that

$$\bar{s}^I_i(t) = \bar{d}^F_i(t)\left(1 - x^I_i(t)\right) \tag{24}$$

Similarly to the case of functional integrity, in order to dynamically assign quantities $x^I_{(h,i)}(t)$ needed in (21), $\forall (h, i) \in \mathcal{E}^s$, first introduce the unbuffered switching signal

$$\rho^I_{(h,i)}(t) = \begin{cases} 0 & \text{if } l_{(h,i)}(t) > \bar{l}_{(h,i)} \\ 1 & \text{otherwise} \end{cases} \tag{25}$$

where $\bar{l}_{(h,i)} \geq 0$ is the *inoperability propagation threshold* of edge $(h, i) \in \mathcal{E}^s$, determining the minimum amount of disservice of node h able to trigger edge inoperability.

The activation of mode 0 represents the precondition for disservice propagation from node h to node i. Indeed, also in this case we consider a buffered switching

signal

$$\theta^I_{(h,i)}(t) = \begin{cases} 0 & \text{if } \begin{pmatrix} \left(\theta^I_{(h,i)}(t^-)=1\right)\wedge \\ \left(\rho^I_{(h,i)}(t-\tau)=0,\ \forall\tau\in[0\ ..\ \tau^b_{(h,i)}]\right) \end{pmatrix} \\ 1 & \text{if } \begin{pmatrix} \left(\theta^I_{(h,i)}(t^-)=0\right)\wedge \\ \left(\rho^I_{(h,i)}(t-\tau)=1,\ \forall\tau\in[0\ ..\ \tau^r_{(h,i)}]\right) \end{pmatrix} \\ \theta^I_{(h,i)}(t^-) & \text{otherwise} \end{cases} \tag{26}$$

where $\tau^b_{(h,i)}, \tau^r_{(h,i)} \in \mathbb{N}_0$ are the *edge buffering time* and *edge recovery response time* associated to $(h,i) \in \mathcal{E}^s$, respectively.

Next, introduce the following edge-based definitions, $\forall (h,i) \in \mathcal{E}^s$:

- *I-type intensity modulation*, i.e.

$$\psi^I_{(h,i)}(t) = \begin{cases} \left(\frac{l_{(h,i)}(t)}{\bar{d}_{(h,i)}(t)}\right)^{\mu_{(h,i)}} & \text{if } \begin{pmatrix} \theta^I_{(h,i)}(t)=0\wedge \\ \bar{d}_{(h,i)}(t)>0 \end{pmatrix} \\ 0 & \text{otherwise} \end{cases} \tag{27}$$

  where $\mu_{(h,i)} > 0$ is an *inoperability dependence sensitivity* parameter, that allows to shape the disservice propagation relationships;

- *I-type time modulation*, described by a set of continuous, monotone decreasing functions $\xi^I_{(h,i),k}(\cdot) : \mathbb{R} \mapsto \mathbb{R}$ with $|\xi^F_{i,k}(x)| \in [0, |x|]$, for $k = 0, 1$ and $\forall x \in \mathbb{R}$.

Then, we can compute edge inoperability through the following formula, $\forall (h,i) \in \mathcal{E}^s$ and $\forall t \in \mathcal{T}$:

$$x^I_{(h,i)}(t) = x^I_{(h,i)}(t^-) + \xi^I_{(h,i),\theta^I_{(h,i)}(t^-)}\left(x^I_{(h,i)}(t^-) - \psi^I_{(h,i)}(t^-)\right) \tag{28}$$

4.1.3. Service, losses and margins

The computational chain illustrated so far leads to the evaluation of effective service capacity $\bar{s}^I(t)$. On this basis, service supply is computed as follows:

$$s(t) = \min\left(d(t), \bar{s}^I(t)\right) \tag{29}$$

where $d(t)$ results from the demand module. Moreover, final and process service terms can be obtained from $s(t)$ by applying the service disaggregation rules introduced in (5) and (6).

Then, service losses can be evaluated by means of (7) and (8). Finally, node i's *service margin* at time $t \in \mathcal{T}$ serves to compare the currently attainable service and demand. In particular, we define it as

$$m_i(t) = \begin{cases} \bar{s}^F_i(t) - d_i(t) & \text{if } x^I_i(t) = 0 \\ \bar{s}^I_i(t) - d_i(t) & \text{otherwise} \end{cases} \tag{30}$$

Here, in the absence of inoperability,

- $m_i(t) > 0$ indicates node i's potential to accommodate further demand, subject to the coping capabilities of the relevant upstream services.

- $m_i(t) \leq 0$ points out a balance or lack of intrinsic service capacity with respect to demand.

Differently, when inoperability is present, the effective service capacity is taken into account, so that $m_i(t) < 0$.

4.2. Demand module

In the DMCI-e framework, the assignment of a demand profile $d(t)$, $\forall t \in \mathcal{T}$, requires to simultaneously consider final demand, process dependencies, and constraints on the service network's capabilities. The demand module performs this task dynamically, adapting demand to the operational conditions of the system. This is done starting from a *reference final service demand* profile $d^{f,*}(t)$, $\forall t \in \mathcal{T}$, assigned as an independent variable, and introducing the following processing components:

- a *final demand assignment* submodule (including external and internal shift mechanisms), which computes final demand $d^f(t)$ from $d^{f,*}(t)$, $\forall t \in \mathcal{T}$, by possibly redistributing demand quotas to fit the current status of services;

- a *process demand assignment* submodule, which outputs the intrinsic capacity-constrained demand terms and the overall node demand $d(t)$, $\forall t \in \mathcal{T}$, based on $d^f(t)$ and $\bar{s}^F(t)$.

Ultimately, as illustrated above, the resulting demand layout is fed into the inoperability submodule, as well as exploited to quantify losses and service margins. Observe that $d^{f,*}(\cdot)$ may embed external perturbations to final demand and that, in this paper, we do not consider feedback mechanisms between service variables and reference demand profiles.

Below in this section, we detail the internal structure and articulation of the mentioned demand submodules.

4.2.1. Final demand assignment

The objective of this submodule is the assignment of final demand $d^f(t)$ starting from $d^{f,*}(t)$, $\forall t \in \mathcal{T}$. When the reference final demand clashes with the current service capabilities, the submodule selects among the alternative final demand assignments that are feasible, based on set criteria. This task is fulfilled by shifting demand quotas from node to node. To this end, in this paper we consider two different final demand shift mechanisms:

- *external shift (ES) of demand*, describing the diversion of some part of a node's reference final demand to other nodes under the action of external drivers (e.g. end customers switching to a different utility operator or means of transport because of disservice);
- *internal shift (IS) of demand*, which results from the activation of internal mechanisms within the service network (e.g. emergency cooperation among operators, exploiting spare service capacities).

Accordingly, we introduce simple graphs $\mathcal{G}^{ES} = (\mathcal{N}, \mathcal{E}^{ES})$ (*external demand shift graph*) and $\mathcal{G}^{IS} = (\mathcal{N}, \mathcal{E}^{IS})$ (*internal demand shift graph*), wherein edge sets $\mathcal{E}^{ES}$ and $\mathcal{E}^{IS}$ determine the demand shifts allowed per mechanism. Therefore, these graph structures can reflect the options in place for substitution among end-customer services.

Under the action of the mentioned shift mechanisms, *final service demand* will be computed from $d_i^{f,*}(t)$ as follows, $\forall i \in \mathcal{N}$ and $\forall t \in \mathcal{T}$:

$$d_i^f(t) = d_i^{f,*}(t) + d_i^{ES}(t) + d_i^{IS}(t) \tag{31}$$

where

$$d_i^{ES}(t) = d_{in,i}^{ES}(t) - d_{out,i}^{ES}(t) \tag{32}$$

$$d_i^{IS}(t) = d_{in,i}^{IS}(t) - d_{out,i}^{IS}(t) \tag{33}$$

denote the external and internal shift components, respectively. Below in this section, terms $d_{in,i}^{ES}(t)$, $d_{out,i}^{ES}(t)$, $d_{in,i}^{IS}(t)$, and $d_{out,i}^{IS}(t)$ appearing therein will be specified.

Finally, we define unfeasible demand

$$d_i^u(t) = \max\left(0, d_i^{f,*}(t) - \bar{s}_i^F(t)\right) \tag{34}$$

and the amount of demand candidate to shift as

$$d_i^{shift}(t) \in \left[d_i^u(t), d_i^{f,*}(t)\right] \tag{35}$$

Thus, the unfeasible demand term takes into account the hard constraint imposed by a node's intrinsic service capacity, while $d_i^{shift}(t)$ can be determined considering additional factors such as the inoperability observed at past steps, possibly adding complexity to the scheme in Figure 1.

ES-type demand shift. As a starting point, introduce outbound demand terms

$$d_{out,i}^{ES}(t) = \begin{cases} k_i^{ES} d_i^{shift}(t) & \text{if } \lambda_i^{ES}(t) \\ 0 & \text{otherwise} \end{cases} \tag{36}$$

$\forall i \in \mathcal{N}$, where $k_i^{ES} \in [0,1]$ is the *ES-type shift ratio* and

$$\lambda_i^{ES}(t) = \lambda_{i,1}^{ES} \wedge \left(\lambda_{i,2}^{ES}(t) \vee \lambda_{i,3}^{ES}(t)\right) \tag{37}$$

with

$$\lambda_{i,1}^{ES} = \left(\mathcal{N}_i^+(\mathcal{G}^{ES}) \neq \emptyset\right) \tag{38}$$

$$\lambda_{i,2}^{ES}(t) = \left(l_i(t-\tau) > 0,\ \forall \tau \in [1\ ..\ \tau_i^{ES}]\right) \tag{39}$$

$$\lambda_{i,3}^{ES}(t) = \left(\lambda_i^{ES}(t^-) \wedge d_i^{shift}(t) > 0\right) \tag{40}$$

Herein, $\tau_i^{ES} \in \mathbb{N}$ is the *ES-type disservice tolerance time* preceding the actual demand shift.

The corresponding ES-type inbound demand terms are

$$d_{in}^{ES}(t) = D^{ES}\, d_{out}^{ES}(t) \tag{41}$$

Herein, the *ES-type demand shift matrix* D^{ES} is defined as follows, $\forall i, j \in \mathcal{N}$:

$$D_{(j,i)}^{ES} = \begin{cases} D_{(j,i)}^{ES,*} & \text{if } j \in \mathcal{N}_i^+(\mathcal{G}^{ES}) \\ 0 & \text{otherwise} \end{cases} \tag{42}$$

with $D_{(j,i)}^{ES,*} \geq 0$. It is assumed that $D^{ES,*} = Z^{ES} \odot \bar{D}^{ES,*}$, where Z^{ES} embeds conversion factors between demand terms and $\bar{D}^{ES,*}$ contains weighting factors determining the demand split. Here, $Z_{(j,i)}^{ES}, \bar{D}_{(j,i)}^{ES,*} \geq 0$, $\forall (i,j) \in \mathcal{E}^{ES}$, while $Z_{(j,i)}^{ES}, \bar{D}_{(j,i)}^{ES,*} = 0$ otherwise. Moreover, $\sum_{j \in \mathcal{N}} \bar{D}_{(j,i)}^{ES,*} = 1$, so that all ES-type outbound demand is reassigned.

IS-type demand shift. Similarly to the previous case, introduce the following definition of IS-type outbound demand terms, for each node $i \in \mathcal{N}$:

$$d_{out,i}^{IS}(t) = \begin{cases} k_i^{IS} d_i^{shift}(t) & \text{if } \lambda_i^{IS}(t) \\ 0 & \text{otherwise} \end{cases} \tag{43}$$

where $k_i^{IS} \in [0,1]$ is the *IS-type shift ratio* and

$$\lambda_i^{IS}(t) = \lambda_{i,1}^{IS}(t) \wedge \left(\lambda_{i,2}^{IS}(t) \vee \lambda_{i,3}^{IS}(t)\right) \tag{44}$$

with

$$\lambda_{i,1}^{IS}(t) = \left(\mathcal{N}_{i,m(t^-)}^+(\mathcal{G}^{IS}) \neq \emptyset\right) \tag{45}$$

$$\lambda_{i,2}^{IS}(t) = \left(l_i(t-\tau) > 0,\ \forall \tau \in [1\ ..\ \tau_i^{IS}]\right) \tag{46}$$

$$\lambda_{i,3}^{IS}(t) = \left(\lambda_i^{IS}(t^-) \wedge d_i^{shift}(t) > 0\right) \tag{47}$$

Herein,

$$\mathcal{N}_{i,m(t)}^+(\mathcal{G}^{IS}) = \left\{j \in \mathcal{N}_i^+(\mathcal{G}^{IS}) : m_{(j,i)}^{IS}(t) > 0\right\} \tag{48}$$

where $m^{IS}_{(j,i)}(t) = m_j(t) + d^{IS}_{(j,i)}(t)$ and $d^{IS}_{(j,i)}(t)$ denotes the demand transferred from node i to node j by the IS-type demand shift mechanism at time t. Moreover, $\tau^{IS}_{(i,j)} \in \mathbb{N}$ denotes the *IS-type disservice tolerance time* preceding the actual demand shift. Observe that, differently from the case in (37), the first logical condition in (44) accounts for the service margins of neighboring nodes, so that demand shift depends on the operating conditions of the network.

Moreover, introduce the IS-type inbound demand shifts:

$$d^{IS}_{in}(t) = D^{IS}(t) d^{IS}_{out}(t) \tag{49}$$

Here, $D^{IS}(t)$ is the *IS-type demand shift matrix*, whose elements will be assigned as

$$D^{IS}_{(j,i)}(t) = \begin{cases} D^{IS,*}_{(j,i)}(t) & \text{if } j \in \mathcal{N}^{+}_{i,m(t^-)}(\mathcal{G}^{IS}) \\ 0 & \text{otherwise} \end{cases} \tag{50}$$

$\forall i, j \in \mathcal{N}$, with $D^{IS,*}(t) = Z^{IS} \odot \bar{D}^{IS,*}(t)$. Similarly to the previous case, Z^{IS} and $\bar{D}^{IS,*}(t)$ describe conversion and weighting factors, respectively, and fulfill analogous sign conditions. Within the IS-type demand shift mechanism, however, we assign weights as follows, $\forall i \in \mathcal{N}$ and $\forall j \in \mathcal{N}^{+}_{i,m(t^-)}(\mathcal{G}^{IS})$:

$$\bar{D}^{IS,*}_{(j,i)}(t) = \frac{m^{IS}_{(j,i)}(t^-)}{\sum_{k \in \mathcal{N}^{+}_{i,m(t^-)}(\mathcal{G}^{IS})} m^{IS}_{(k,i)}(t^-)} \tag{51}$$

This implies that, also in this case, all the outbound demand is reassigned, based on a criterion of proportionate demand redistribution to downstream nodes with respect to a service margin measure and subject to the logic in (44).

Remark 2. ***(Comparison of ES- and IS-type demand shift mechanisms)*** *In ES-type demand shift logic, coefficients $D^{ES}_{(i,j)}$ may be used to describe service preferences according to external criteria. In contrast, the IS-type mechanism determines demand redistribution in the awareness of neighboring nodes' service status.*

Remark 3. ***(Shift ratios)*** *A choice of shift ratios $k^{IS}_i \in [0,1]$ and $k^{ES}_i \in [0,1]$ such that $k^{IS}_i + k^{ES}_i \leq 1$ ensures that the two mentioned demand shift mechanisms don't overlap, irrespective of the activation of the corresponding logical conditions. This means that the outbound demand assigned to node i through the two mechanisms won't exceed the amount of demand candidate to shift. Depending on the application, this property may simply be ensured by assuming that $\nexists j,k \in \mathcal{N} : (i,j) \in \mathcal{E}^{IS} \wedge (i,k) \in \mathcal{E}^{ES}$, $\forall i \in \mathcal{N}$, so that each node has a single active demand shift mechanism.*

4.2.2. Process demand assignment

Starting from final demand $d^f(t)$, provided by the final demand assignment submodule, here we characterize the process demand it generates and the overall service demand $d(t)$, $\forall t \in \mathcal{T}$. Moving from the demand disaggregation procedure detailed in Subsection 3.2, here the service constraints generated by the functional integrity loss submodule are taken into account. To this end, $\forall t \in \mathcal{T}$, define the *intrinsic capacity-constrained demand*

$$\bar{d}^F(t) = \min\left(d(t), \bar{s}^F(t)\right) \tag{52}$$

i.e. the part of demand $d(t)$ that does not exceed the intrinsic service capacity of nodes. Then, (11) is replaced by

$$d(t) = d^f(t) + \Delta \bar{d}^F(t) \tag{53}$$

equivalently

$$d_i(t) = d^f_i(t) + \sum_{j \in \mathcal{N}^{+}_i(\mathcal{G}^s)} d_{(i,j)}(t), \ \forall i \in \mathcal{N} \tag{54}$$

where

$$d_{(i,j)}(t) = \Delta_{(i,j)} \bar{d}^F_j(t), \ \forall (i,j) \in \mathcal{E}^s \tag{55}$$

and Δ is plausible with respect to $\bar{d}^F(t)$.

The process demand assignment submodule solves (52) and (53) for $\bar{d}^F(t)$ and $d(t)$, computes $d_{(i,j)}(t)$, $\forall (i,j) \in \mathcal{E}^s$, and feeds the results into the service module. Observe that (52) and (53) enforce consistency between process demand assignment and the demand disaggregation and aggregation rules laid down for the system, even when the above-mentioned service constraints are active.

Remark 4. ***(Standard demand profiles)*** *A demand profile $d(t)$ generated through the DMCI-e is qualified as a standard demand profile when, being specified assuming $d^f(t) = d^{f,*}(t)$ and no service perturbation in place, it fulfills $d(t) \leq \bar{s}^{MAX}$, $\forall t \in \mathcal{T}$. In our illustrative examples, standard demand profiles will serve to describe a feasible nominal service request and subsequently evaluate the performance of the system under non-nominal conditions.*

5. Illustrative examples

We consider a system of seven nodes composing the service graph $\mathcal{G}^s$ illustrated in Figure 2. Terminal nodes 1, 2 and 3 operate as either β- or γ-type and share 7 as a common in-neighbor. The rest of nodes in the network are α-type. In particular, the following arrangements will be studied over $\mathcal{T} = [0 \,..\, 100]$:

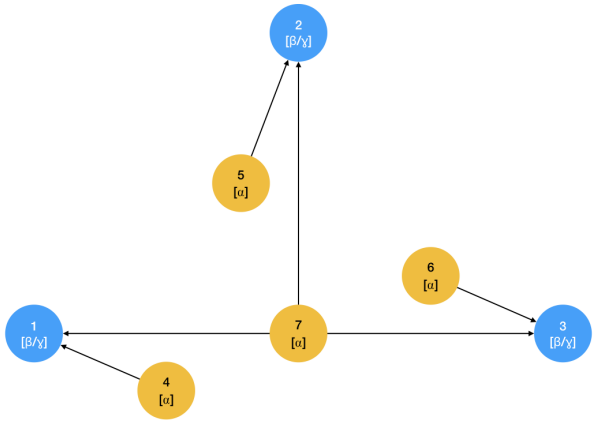

Figure 2: service graph $\mathcal{G}^s$ for the illustrative examples.

- β-configuration: $\nu_i = \beta$, $i = 1, 2, 3$;
- γ-configuration: $\nu_i = \gamma$, $i = 1, 2, 3$.

The service network is assumed to start from a fully operational regime with no demand shift in place, and it is characterized by the following parameters:

- $\tau_i^b, \tau_i^r = 0, \xi_{i,0}^F(x) = -0.5x, \xi_{i,1}^F(x) = -0.2x, \forall i \in \mathcal{N}$;
- $\bar{l}_{(i,j)}, \tau_{(i,j)}^b, \tau_{(i,j)}^r = 0$, $\mu_{(i,j)} = 1$, $\xi_{(i,j),0}^I(x) = -0.5x$, $\xi_{(i,j),1}^I(x) = -0.2x$, $\forall (i,j) \in \mathcal{E}^s$;
- $$A = \begin{bmatrix} 0 & 0 & 0 & 0 & 0 & 0 & 0 \\ 0 & 0 & 0 & 0 & 0 & 0 & 0 \\ 0 & 0 & 0 & 0 & 0 & 0 & 0 \\ 1/2 & 0 & 0 & 0 & 0 & 0 & 0 \\ 0 & 3/4 & 0 & 0 & 0 & 0 & 0 \\ 0 & 0 & 1/4 & 0 & 0 & 0 & 0 \\ 1/2 & 1/4 & 3/4 & 0 & 0 & 0 & 0 \end{bmatrix}$$

  and Δ computed according to (15).

The remaining model attributes will be assigned below on a per-case basis. Finally, reference demand profiles are chosen as $d^{f,*}(t) = [1\ 1\ 1\ 0\ 0\ 0\ 0]'$, $\forall t$. Thus, under nominal conditions, the first three nodes serve final demand, whilst the others supply process demand.

Next, we discuss performance aspects of the system, in its different configurations, when the demand shift mechanisms are either inactive or active.

5.1. System with inactive demand shift

As a first step, demand shift mechanisms are considered as inactive, so that $d^f(\cdot) = d^{f,*}(\cdot)$. Correspondingly, when solving (12) for $d(t)$, we obtain, $\forall t \in \mathcal{T}$:

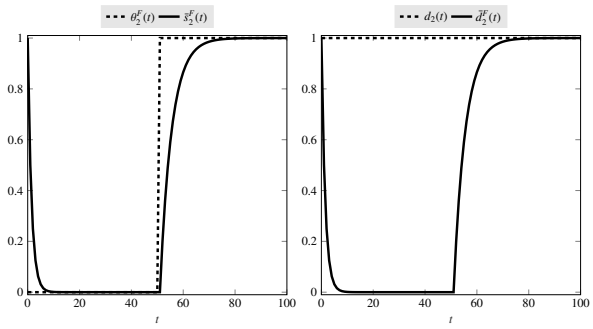

Figure 3: node 2's buffered switching signal $\theta_2^F(t)$ and resulting intrinsic service capacity $\bar{s}_2^F(t)$ (left plot); node 2's demand $d_2(t)$ and intrinsic capacity-constrained demand $\bar{d}_2^F(t)$ (right plot).

- β-configuration: $d(t) = [1\ 1\ 1\ 1\ 1\ 1\ 3]'$;
- γ-configuration: $d(t) = [1\ 1\ 1\ 2\ 4/3\ 4\ 22/3]'$.

For each configuration, $\bar{s}^{MAX}$ is fixed to match exactly the (constant) demand indicated above. Accordingly, along the lines of Remark 4, in both cases $d(t)$ constitutes a standard demand profile.

Referring to the proposed configurations, next we illustrate some key features of the model.

5.1.1. Functional integrity loss and intrinsic capacity-constrained demand

We consider the system in β-configuration and a perturbation affecting node 2 over threat impact times $\mathcal{T}_2^F = [0\ ..\ 50]$ and F-type regime functional integrity reduction $\bar{\psi}_2^F = 1$. Under this parameterization, functional integrity loss dynamically affects node 2's intrinsic service capacity $\bar{s}_2^F(t)$ and, consequently, the intrinsic capacity-constrained demand term $\bar{d}_2^F(t)$, as illustrated in Figure 3. Accordingly, we have a demand reduction in upstream nodes 5 and 7, see Figure 4. Observe that node 7 keeps serving nodes 1 and 3 at nominal demand levels. Moreover, service margin $m_5(t), m_7(t) \geq 0$, $\forall t \in \mathcal{T}$, and in particular they rise corresponding to the reduction phase of downstream process demand from node 2. As a consequence, service loss only manifests at node 2, as a product of its intrinsic functional integrity loss.

5.1.2. Inoperability in β- and γ-type nodes

In this case, we consider a functionality perturbation on node 5, with $\mathcal{T}_5^F = [1\ ..\ 50]$ and $\bar{\psi}_5^F = 1$. The latter, under the considered model parameterization, induces inoperability in the system. In particular, we focus on how service of node 2 is affected, depending on node types.

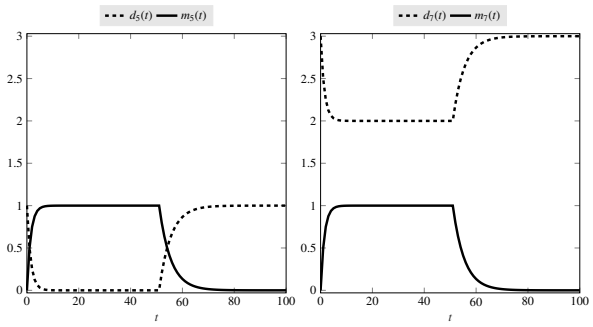

Figure 4: node 5's demand $d_5(t)$ and service margin $m_5(t)$ (left plot); node 7's demand $d_7(t)$ and service margin $m_7(t)$ (right plot).

- β-configuration: the complete service loss of node 5 induces only a partial inoperability in node 2, tanks to the availability of node 7. Therefore, it does not prevent node 2 from delivering some service, see Figure 5.

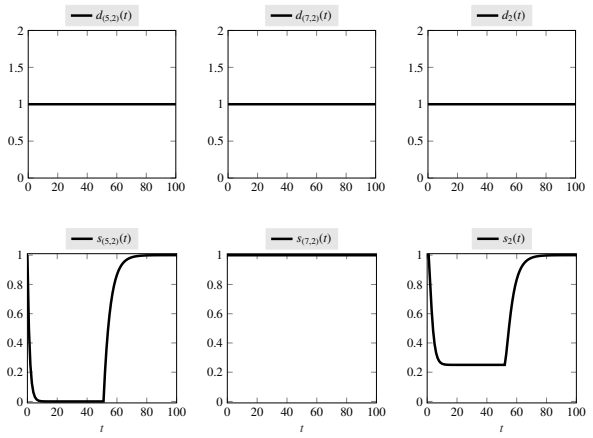

Figure 5: service perturbation propagation in β-configuration.

- γ-configuration: differently from the previous case, here the services by node 2's in-neighbors represent non-substitutable factors, thus the disservice of node 5 can fully compromise the end-customer supply by node 2, as illustrated in Figure 6.

5.2. *System with active demand shift*

As a next step, we consider the same system as in Subsection 5.1.1, with the following exceptions:

- $\bar{s}_3^{MAX}, \bar{s}_6^{MAX} = 2$, which allows end-customer service provider node 3 to have spare service capacity;

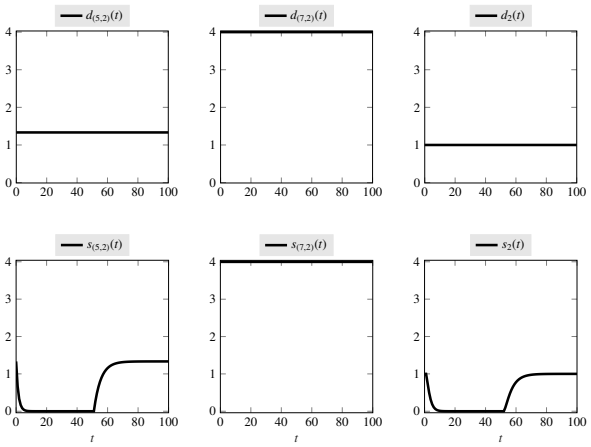

Figure 6: service perturbation propagation in γ-configuration.

- either an ES- or IS-type demand shift mechanism in place, where $\mathcal{G}^{ES}$ and $\mathcal{G}^{IS}$ have identical structure (see Figure 7), while $\tau_2^{ES}, \tau_2^{IS} = 10$, $d^{shift}(t) = d^u(t)$, $\forall t \in \mathcal{T}$, and

$$D^{ES} = \begin{bmatrix} 0 & 1/2 & 0 & 0 & 0 & 0 & 0 \\ 0 & 0 & 0 & 0 & 0 & 0 & 0 \\ 0 & 1/2 & 0 & 0 & 0 & 0 & 0 \\ 0 & 0 & 0 & 0 & 0 & 0 & 0 \\ 0 & 0 & 0 & 0 & 0 & 0 & 0 \\ 0 & 0 & 0 & 0 & 0 & 0 & 0 \\ 0 & 0 & 0 & 0 & 0 & 0 & 0 \end{bmatrix} \tag{56}$$

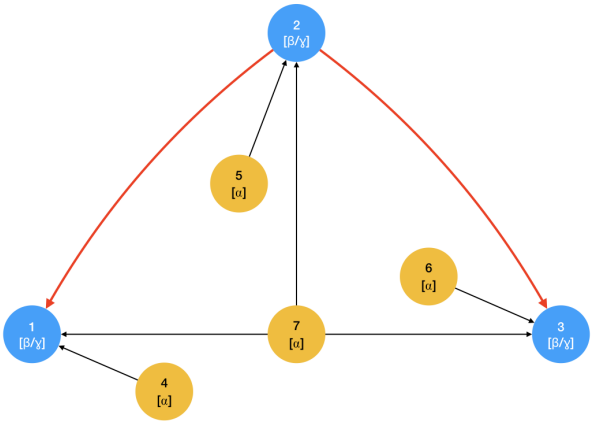

Figure 7: demand shift graphs $\mathcal{G}^{ES}$ and $\mathcal{G}^{IS}$ (identical, in red).

Also in this example, we focus on two different situations, characterized by the exclusive presence of one or the other demand shift mechanism.

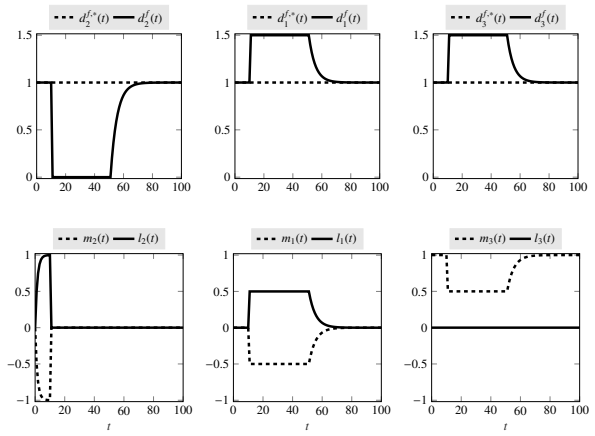

Figure 8: reference and final demand profiles for terminal nodes (top row), service margins and service losses for terminal nodes (bottom row) under the ES-type demand shift.

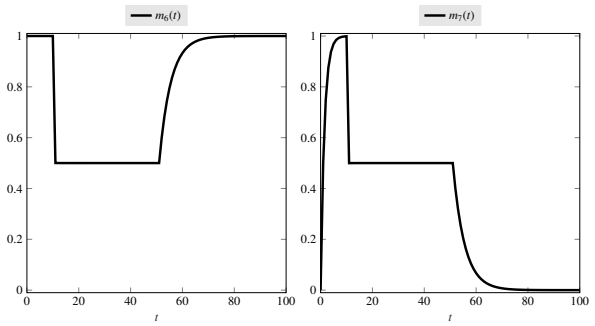

Figure 9: service margin of node 3's service graph in-neighbors under the ES-type demand shift.

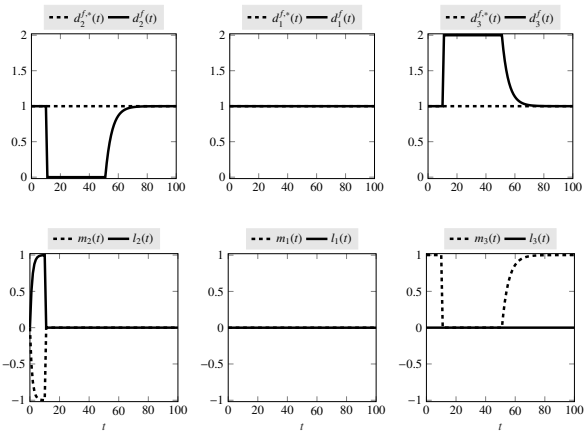

Figure 10: reference and final demand profiles for terminal nodes (top row), service margins and service losses for terminal nodes (bottom row) under the IS-type demand shift.

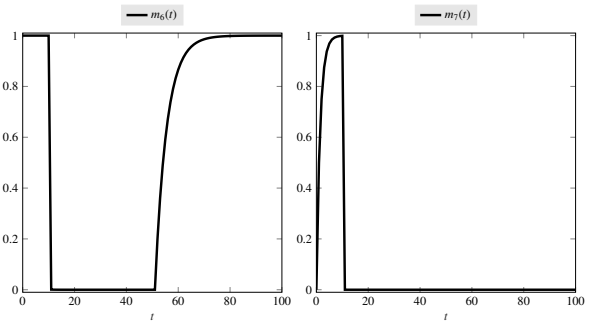

Figure 11: service margin of node 3's service graph in-neighbors under the IS-type demand shift.

5.2.1. ES-type demand shift

In this case, we assume $k_2^{ES} = 1$ and $k_2^{IS} = 0$. Considering the structure of D^{ES}, after the disservice tolerance time τ_2^{ES} demand $d_{out,2}^{ES}(t)$ is equally distributed between nodes 1 and 3, as illustrated in Figure 8. In node 1, considering that $\bar{s}_1^{MAX} = 1$, the presence of zero service margin doesn't allow the incoming shifted demand to be served, which implies the emergence of service loss. On the other side, node 3 is able to maintain a zero service margin balance, without service loss, thanks to the values assigned to $\bar{s}_3^{MAX}$ and $\bar{s}_6^{MAX}$ jointly with the fact that service resources at the level of node 7 are made free by the disservice status of node 2, see Figure 9.

5.2.2. IS-type demand shift

Conversely, when we consider the case with $k_2^{ES} = 0$ and $k_2^{IS} = 1$, demand reallocation depends on service margin. As a consequence, since node 1 has zero service margin while node 3 does, the whole $d_{out,2}^{IS}(t)$ is allocated to the latter. Ultimately, the system is able fully serve the reallocated demand, as illustrated in Figures 10 and 11.

6. Conclusions

According to review paper [16], the DMCI formalism proposed in [1] belongs to the category of flow-based network models. DMCI enables the performance assessment of interdependent systems using some high-level, sector-agnostic semantics (such as service capacity, service demand, inoperability, etc.).

In the present study, we further enhanced the capabilities of DMCI with the primary objective of making it fully applicable to the analysis of multi-sectoral CI systems (e.g. coupled and transportation infrastructures). The evolved DMCI framework (DMCI-e) in-

cludes a broader set of node types used to represent service aggregation/demand disaggregation modes, as well as multiple demand shift mechanisms. The moderate data requirements of the model render DMCI-e feasible for application in decision- and policy-making contexts, especially in cooperation with operators.

Three key areas for perspective development and application of DMCI-e are outlined below.

- *Model formulation and validation*. Options exist to further extend the mathematical foundation and capabilities of the model itself. For instance, the addition of more complex failure and recovery mechanisms can be envisaged to represent more accurately the impact of specific threat scenarios on infrastructure nodes. However, this might come at the expense of user-friendliness and simplicity of the model. In addition, a more extensive treatment of a node's vulnerability and functional integrity could be achieved through a comprehensive classification of different types of threats and hazards; to this end, empirical methods for CI vulnerability and interdependence analysis could be extremely useful [18, 19, 20, 55]. Finally, future work includes the validation of the DMCI-e framework in applications, especially through case studies involving multi-domain infrastructures.

- *Model federation*. The second development area is related to the federation of DMCI-e with other modeling techniques, combining different levels of abstraction. In this sense, an option is to let engineering-based models with a sector focus provide input to DMCI-e in terms of functional integrity loss (e.g. fragility models) or inoperability (e.g. network flow models). Similarly, DMCI-e may provide input to further analysis layers. As a consequence, DMCI-e may play a role as a platform able to integrate many other models, in order to have a full-fledged analysis framework that synergizes high-level representations with domain-specific modeling methodologies from particular application areas.

- *Stakeholder engagement and field use*. DMCI-e can be considered as a means to facilitate interaction among CI stakeholders. The use of the proposed modeling framework in the context of public-private partnerships for CI protection and resilience may facilitate information sharing among operators on a service-oriented basis and enable large-scale simulation-backed analyses. Recent applications of the DMCI model suggest considerable potential in this direction [1, 56, 57]. Besides, an interesting option lies in linking the simulation model with real-time decision-making and resilience building in CI systems. This includes its exploitation in defining response strategies, supporting emergency services, enhancing post-event analysis, and reporting.

Acknowledgements

The work presented in this paper has been developed within MATRICS (`www.matrics.it`), a research project jointly co-funded by the Italian Ministry of Research and Education (MIUR) and the Lombardy Region Government (Italy), as well as within the CIPS program (Prevention, Preparedness and Consequence Management of Terrorism and other Security-related Risks) funded by DG HOME. The financial support is gratefully acknowledged. The authors would also like to thank Mr. Nelson Carreras for his contribution during the early development phases of this work.

[1] P. Trucco, E. Cagno, M. De Ambroggi, Dynamic functional modelling of vulnerability and interoperability of Critical Infrastructures, Reliability Engineering & System Safety 105 (2012) 51–63.

[2] B. Robert, M.-H. Senay, M.-È. P. Plamondon, J.-P. Sabourin, Characterization and ranking of links connecting life support networks, Canada Public Safety, 2002.

[3] H. Luiijf, H. Burger, M. Klaver, H. Marieke, Critical infrastructure protection in the Netherlands: A Quick-scan, Copenhagen, Denmark: EICAR Denmark, 2003.

[4] P. Pederson, D. Dudenhoeffer, S. Hartley, M. Permann, Critical infrastructure interdependency modeling: a survey of US and international research, Idaho National Laboratory 25 (2006) 27.

[5] T. D. O'Rourke, Critical infrastructure, interdependencies, and resilience, BRIDGE-Washington-National Academy of Engineering 37 (1) (2007) 22.

[6] D. L. Alderson, J. C. Doyle, Contrasting views of complexity and their implications for network-centric infrastructures, IEEE Transactions on systems, man, and cybernetics-Part A: Systems and humans 40 (4) (2010) 839–852.

[7] K. Gopalakrishnan, S. Peeta, Sustainable and resilient critical infrastructure systems: simulation, modeling, and intelligent engineering, Springer, 2010.

[8] S. Hallegatte, J. Rentschler, J. Rozenberg, Lifelines, Washington, DC: World Bank, 2019.

[9] S. M. Rinaldi, J. P. Peerenboom, T. K. Kelly, Identifying, understanding, and analyzing critical infrastructure interdependencies, IEEE Control Systems 21 (6) (2001) 11–25.

[10] G. Pescaroli, M. Nones, L. Galbusera, D. Alexander, Understanding and mitigating cascading crises in the global interconnected system, International Journal of Disaster Risk Reduction 30 (2018) 159–163.

[11] M. Theocharidou, L. Galbusera, G. Giannopoulos, Resilience of critical infrastructure systems: Policy, research projects and tools, in: B. D. Trump, M.-V. Florin, I. Linkov (Eds.), IRGC Resource Guide on Resilience (vol. 2): Domains of resilience for complex interconnected systems, EPFL International Risk Governance Center (IRGC), Lausanne, CH, 2018.

[12] Council Directive 2008/114/EC of 8 December 2008 on the identification and designation of European critical infrastructures and the assessment of the need to improve their protection, Official Journal of the European Union L 345 (23.12.2008) 75–82, https://eur-lex.europa.eu/eli/dir/2008/114/oj.

[13] European Commission, Commission Staff Working Document on a new approach to the European Programme for Critical Infrastructure Protection: Making European Critical Infrastructures more secure SWD(2013) 318 final, http://ec.europa.eu/transparency/regdoc/rep/10102/2013/EN/10102-2013-318-EN-F1-1.PDF.

[14] Directive (EU) 2016/1148 of the European Parliament and of the Council of 6 July 2016 concerning measures for a high common level of security of network and information systems across the Union, Official Journal of the European Union L 194 (19.7.2016) 1–30, https://eur-lex.europa.eu/eli/dir/2016/1148/oj.

[15] L. Galbusera, G. Giannopoulos, Leveraging network theory and stress tests to assess interdependencies in critical infrastructures, in: Critical Infrastructure Security and Resilience, Springer, 2019, pp. 135–155.

[16] M. Ouyang, Review on modeling and simulation of interdependent critical infrastructure systems, Reliability engineering & System safety 121 (2014) 43–60.

[17] P. Trucco, M. De Ambroggi, P. F. Campos, I. Azzini, G. Giannopoulos, Extension of DMCI to heterogeneous infrastructures: model and pilot application, in: Probabilistic Safety Assessment and Management PSAM 12, 2014.

[18] B. C. Ezell, J. V. Farr, I. Wiese, Infrastructure risk analysis model, Journal of Infrastructure Systems 6 (3) (2000) 114–117.

[19] B. C. Ezell, J. V. Farr, I. Wiese, Infrastructure risk analysis of municipal water distribution system, Journal of Infrastructure Systems 6 (3) (2000) 118–122.

[20] B. Robert, A method for the study of cascading effects within lifeline networks, International Journal of Critical Infrastructures 1 (1) (2004) 86–99.

[21] D. C. Barton, E. D. Edison, D. A. Schoenwald, R. G. Cox, R. K. Reinert, Simulating economic effects of disruptions in the telecommunications infrastructure, Report no. SAND2004-0101. January.

[22] T. Brown, W. Beyeler, D. Barton, Assessing infrastructure interdependencies: the challenge of risk analysis for complex adaptive systems, International Journal of Critical Infrastructures 1 (1) (2004) 108–117.

[23] A. Rose, G. Oladosu, S.-Y. Liao, Regional economic impacts of terrorist attacks on the electric power system of Los Angeles: a computable general disequilibrium analysis, in: Second Annual Symposium of the DHS Center for Risk and Economic Analysis of Terrorism Events, USC, Los Angeles, CA, August, 2005.

[24] V. Rosato, L. Issacharoff, F. Tiriticco, S. Meloni, S. Porcellinis, R. Setola, Modelling interdependent infrastructures using interacting dynamical models, International Journal of Critical Infrastructures 4 (1-2) (2008) 63–79.

[25] M. Ouyang, L. Hong, Z.-J. Mao, M.-H. Yu, F. Qi, A methodological approach to analyze vulnerability of interdependent infrastructures, Simulation Modelling Practice and Theory 17 (5) (2009) 817–828.

[26] J. Winkler, L. Dueñas-Osorio, R. Stein, D. Subramanian, Interface network models for complex urban infrastructure systems, Journal of Infrastructure Systems 17 (4) (2011) 138–150.

[27] C. Nan, I. Eusgeld, W. Kröger, Analyzing vulnerabilities between SCADA system and SUC due to interdependencies, Reliability Engineering & System Safety 113 (2013) 76–93.

[28] D. F. Rueda, E. Calle, Using interdependency matrices to mitigate targeted attacks on interdependent networks: A case study involving a power grid and backbone telecommunications networks, International Journal of Critical Infrastructure Protection 16 (2017) 3–12.

[29] C. Zhang, J.-j. Kong, S. P. Simonovic, Restoration resource allocation model for enhancing resilience of interdependent infrastructure systems, Safety science 102 (2018) 169–177.

[30] L. Galbusera, G. Giannopoulos, S. Argyroudis, K. Kakderi, A boolean networks approach to modeling and resilience analysis of interdependent critical infrastructures, Computer-Aided Civil and Infrastructure Engineering 33 (12) (2018) 1041–1055.

[31] E. Zio, Challenges in the vulnerability and risk analysis of critical infrastructures, Reliability Engineering & System Safety 152 (2016) 137–150.

[32] G. Stergiopoulos, E. Vasilellis, G. Lykou, P. Kotzanikolaou, D. Gritzalis, Critical infrastructure protection tools: classification and comparison, in: Proceedings of the 10th International Conference on Critical Infrastructure Protection, USA, Vol. 8, 2016.

[33] M. Ouyang, Z. Wang, Resilience assessment of interdependent infrastructure systems: With a focus on joint restoration modeling and analysis, Reliability Engineering & System Safety 141 (2015) 74–82.

[34] M. Ouyang, Z. Pan, L. Hong, Y. He, Vulnerability analysis of complementary transportation systems with applications to railway and airline systems in China, Reliability Engineering & System Safety 142 (2015) 248–257.

[35] V. V. Lesnykh, V. S. Petrov, T. B. Timofeyeva, Problems of risk assessment in intersystem failures of life support facilities, International Journal of Critical Infrastructures 12 (3) (2016) 213–228.

[36] M. Ouyang, Critical location identification and vulnerability analysis of interdependent infrastructure systems under spatially localized attacks, Reliability Engineering & System Safety 154 (2016) 106–116.

[37] G. Stergiopoulos, P. Kotzanikolaou, M. Theocharidou, G. Lykou, D. Gritzalis, Time-based critical infrastructure dependency analysis for large-scale and cross-sectoral failures, International Journal of Critical Infrastructure Protection 12 (2016) 46–60.

[38] S. Thacker, J. W. Hall, R. Pant, Preserving Key Topological and Structural Features in the Synthesis of Multilevel Electricity Networks for Modeling of Resilience and Risk, Journal of Infrastructure Systems 24 (1) (2018) 04017043.

[39] S. Dunn, S. Wilkinson, Hazard tolerance of spatially distributed complex networks, Reliability Engineering & System Safety 157 (2017) 1–12.

[40] C. Zhao, N. Li, D. Fang, Criticality assessment of urban interdependent lifeline systems using a biased PageRank algorithm and a multilayer weighted directed network model, International Journal of Critical Infrastructure Protection.

[41] G. Stergiopoulos, V. Kouktzoglou, M. Theocharidou, D. Gritzalis, A process-based dependency risk analysis methodology for critical infrastructures, International Journal of Critical Infrastructures 13 (2-3) (2017) 184–205.

[42] S. Thacker, R. Pant, J. W. Hall, System-of-systems formulation and disruption analysis for multi-scale critical national infrastructures, Reliability Engineering & System Safety 167 (2017) 30–41.

[43] Corbet, Thomas F and Beyeler, Walt and Wilson, Michael L and Flanagan, Tatiana P, A model for simulating adaptive, dynamic flows on networks: Application to petroleum infrastructure, Reliability Engineering & System Safety 169 (2018) 451–465.

[44] C. Nan, G. Sansavini, Multilayer hybrid modeling framework for the performance assessment of interdependent critical infrastructures, International Journal of Critical Infrastructure Protec-

tion 10 (2015) 18–33.

[45] E. Ferrario, N. Pedroni, E. Zio, Evaluation of the robustness of critical infrastructures by Hierarchical Graph representation, clustering and Monte Carlo simulation, Reliability Engineering & System Safety 155 (2016) 78–96.

[46] B. Wu, A. Tang, J. Wu, Modeling cascading failures in interdependent infrastructures under terrorist attacks, Reliability Engineering & System Safety 147 (2016) 1–8.

[47] H. Fotouhi, S. Moryadee, E. Miller-Hooks, Quantifying the resilience of an urban traffic-electric power coupled system, Reliability Engineering & System Safety 163 (2017) 79–94.

[48] C. Heracleous, P. Kolios, C. G. Panayiotou, G. Ellinas, M. M. Polycarpou, Hybrid systems modeling for critical infrastructures interdependency analysis, Reliability Engineering & System Safety 165 (2017) 89–101.

[49] X. Liu, J. Zhang, P. Zhu, Modeling cyber-physical attacks based on probabilistic colored Petri nets and mixed-strategy game theory, International Journal of Critical Infrastructure Protection 16 (2017) 13–25.

[50] E. C. Portante, J. A. Kavicky, B. A. Craig, L. E. Talaber, S. M. Folga, Modeling electric power and natural gas system interdependencies, Journal of Infrastructure Systems 23 (4) (2017) 04017035.

[51] D. C. Barton, E. D. Eidson, D. A. Schoenwald, K. L. Stamber, R. K. Reinert, Aspen-EE: an agent-based model of infrastructure interdependency, SAND2000-2925. Albuquerque, NM: Sandia National Laboratories.

[52] K. Sanford Bernhardt, S. McNeil, Agent-based modeling: Approach for improving infrastructure management, Journal of Infrastructure Systems 14 (3) (2008) 253–261.

[53] I. Eusgeld, C. Nan, S. Dietz, "System-of-systems" approach for interdependent critical infrastructures, Reliability Engineering & System Safety 96 (6) (2011) 679–686.

[54] L. Galbusera, G. Giannopoulos, On input-output economic models in disaster impact assessment, International Journal of Disaster Risk Reduction 30 (2018) 186–198.

[55] R. E. Bloomfield, P. Popov, K. Salako, V. Stankovic, D. Wright, Preliminary interdependency analysis: An approach to support critical-infrastructure risk-assessment, Reliability Engineering & System Safety 167 (2017) 198–217.

[56] E. Cagno, P. Trucco, M. De Ambroggi, Interdependency analysis of CIs in real scenarios, Advances in Safety, Reliability and Risk Management: ESREL 2011 (2011) 410.

[57] B. Petrenj, P. Trucco, Simulation-based characterisation of critical infrastructure system resilience, International Journal of Critical Infrastructures 10 (3-4) (2014) 347–374.